OVLBI-ES MEMO NO. 18

A Frequency-Selective Surface for the OVLBI Earth Station: Initial Design and Test Results

Bill Shillue

November 20, 1991

1 General

As reported in OVLBI memo #4 [1], it is necessary for the Green Bank Earth Station to support the following space research allocation bands:

Frequency(GHz)	Direction	Space Research Allocation
7.190-7.235	uplink only	primary
8.450-8.500	downlink only	primary
13.40-15.35	both directions	secondary

Specifically, to support the VSOP and Radioastron projects, the following frequencies must be supported:

Frequency (GHz)	Satellite	Use	Link	Polarization
7.2000 GHz	Radiastron	CW	uplink	RCP
8.4720 GHz	Radiastron	CW	downlink	RCP
14.200 GHz	VSOP	data, 150 MHz	downlink	LCP
15.063 GHz	Radiastron	data, 150 MHz	downlink	RCP
15.300 GHz	VSOP	CW	uplink	LCP

To satisfy the wide bandwidth requirement of the feed and optics on the antenna, an optics scheme was proposed [2], and adopted as our primary option at the OVLBI Earth Station preliminary design review [3]. This scheme proposed to use a frequency-selective-surface (FSS) as the means to split the beam at the secondary focus into an X-band component and a Ku-band component. This memo will discuss the prototype design and testing of the FSS that has been done to date.

2 Specifications

The FSS design needed, at the very least, to be nearly transparent at 8.5 GHz and highly reflective at 14.2 GHz. The close spacing of these two frequencies, a ratio of 1.67:1, meant that many typical FSS element designs such as dipoles, crossed dipoles, patches, or loops could not be used. A gridded square loop element was decided upon because it can diplex frequencies as close as 1.3:1 with little added crosspolarization. A specification, A34200N4, was written and used as a guide in his design. The original specification was as

[1] L.R. D'Addario, "Requirements for the Feed and Optics for the 45 ft. Antenna in Green Bank," OVLBI-ES Memo #4, Sept. 7, 1990

[2] S. Srikanth, "A Possible Optics Scheme for the 45-Foot Antenna in Green Bank," OVLBI-ES Memo #5, Nov. 27, 1990

[3] L.R. D'Addario, B. Shillue, and D. Varney, "The Green Bank OVLBI Earth Station: Preliminary Design," July, 2, 1991

follows:

Band	Frequency (GHz)	Transmission Loss	Reflection Loss
Transmission	7-9 GHz	< .2dB	——
Prime Transmission	7.15-7.28 GHz, 8.34-8.60 GHz	< .05 dB	——
Reflection	13.4-15.4 GHz	> 16.4 dB	< 0.1 dB
Prime Reflection	14.10-14.30 GHz, 14.90-15.40 GHz	> 19.4 dB	< 0.05 dB

Since there was some concern that this specification may not be achievable, we decided that the performance should be optimized for 8.5 GHz, 14.2 GHz, and 15.063 GHz, the downlink frequencies.

3 Design

The first part of the FSS design was determining what the best approach would be. There are three basic types of frequency-selective-surfaces: a thin single-layer FSS, an FSS consisting of multiple layers of copper and dielectric, and a metal-only FSS consisting of a grid of waveguide slots. The second approach would require a complex fabrication and is difficult to model, and the third approach would be prohibitively expensive due to the extensive machining required. Thus, the first approach, a single-layer FSS, was taken due to its inherent simplicity and low material loss.

The next step was to determine what type of element was needed. The frequency response that we required ruled out simple elements with a single resonance. More complex elements that could meet our frequency requirements and that offered low cross-polarization include the Jerusalem-Cross, Gridded Jerusalem-Cross, Double-Square Loop, and Gridded-Square Loop. A consultant from JPL, T.K. Wu, who had computer software that accurately simulated the response of the gridded-square loop FSS, was available to help with the design. Since the gridded-square loop element was also a simple design, and it appeared to be able to meet our requirements, that is the element we selected. It is likely that other element designs would also have worked.

The final design decision was the type of backup structure to use. A previous NRAO FSS design had used a Kevlar honeycomb backup, which is very strong but also lossy. We decided to use a low-loss foam backup structure.

Dr. Wu was responsible for selecting the dimensions of the prototype FSS and running the computer simulations. The FSS was simulated on a Cray X-MP supercomputer at JPL using a computer code developed by Robert Vacchione at the University of Illinois for the design of single layer FSS's with arbitrarily shaped element. The code uses the standard assumption that the FSS is infinite in transverse extent, so that the boundary conditions at the dielectric and copper interfaces need only be solved for a single element, and the results extrapolated according to Floquet's theorem for periodic structures.[4] The dimensions of a single element of this FSS are shown in Fig. 1. The FSS consisted of copper elements etched on a 3-mil Kapton substrate.

The computer code has a limitation in that the element is discretized into 32 x 32 unit cells. This means that if we want to fine-tune the design so that some dimension of the element, width or spacing, is not $\frac{n}{32} * p$, where p is the size of the unit element, and n is an integer from 1 to 32, we must use a less rigorous simulation. Although the element design has 4 degrees of freedom, this limitation is a hindrance because the frequency change resulting from the change in a single unit-cell can be as large as $\Delta f = \frac{1}{32} f_0$ which is equal to 470 MHz if $f_0 = 15$ GHz. Lumped element models for simulation of the gridded square loop based upon work by Lee and Langley[5] were developed as a secondary way of analyzing the FSS.

The computer simulation study of the FSS resulted in the plots shown in Figure 2, showing the transmission of the FSS for plane wave incidence versus frequency, with incident angle as a parameter.

4 Materials

The substrate material used was a 3-mil thick Kapton substrate with a 1 oz. (1.4 mil) copper laminate. Kapton is a material with a good combination of electrical, mechanical, and thermal properties that also

[4] Amitay, Galindo, Wu, "Theory and Analysis of Phased Array Antennas," Wiley Interscience, New York, 1972, Chapter 2, pp. 37-74

[5] Lee, C.K. and Langley, R.J., "Equivalent-Circuit Model¦s for Frequency-Selective Surfaces at Oblique Angles of Incidence, IEE Proc., Pt. H, Oct. 1985, pp. 395–399

performs well at microwave frequencies. It had been used previously in the design of the VLBA FSS at the NRAO. Kapton is a DuPont product, but was purchased in laminated form from Westinghouse Fortin. The foam support material was Rohacell 51 from Rohm-Tech. A similar, more expensive material of lower loss called Eccofoam is available from Emerson and Cuming.

5 Fabrication

Artwork for the gridded-square loop FSS was generated in AutoCad at the NRAO at twice actual size. The HP HP8570B plotter was used, which was able to handle a drawing size of up to 22.75" by 34.375". Because of the tolerance limitations of the plotter, the dimensions of the AutoCad drawing did not correspond exactly to the plotter drawing, so the line widths and lengths in both horizontal and vertical directions were carefully calibrated. The result was that the plotted dimensions at twice size were within 0.5 mils of the desired values after repeated measurement under a microscope. Two plots of dimension 18.4236" x 27.6354" were made and carefully taped together, followed by a photoreduction of the plot done by Ron Monk at the Green Bank photo lab, thus generating the 18.4236" x 13.8177" circuit mask.

The circuit mask is used by a vendor, Precision Prototypes,[6] to fabricate the copper pattern on the Kapton. First, a 16" x 20" Kapton substrate is supplied because the vendor requires a one inch border around the edge of the pattern. The copper-laminated Kapton is spun with photoresist and then baked. Then the resist layer is exposed to light through the mask for a controlled time. The emulsion layer of the mask must be in contact with the resist. The exposed areas of resist are then washed off in a developing solution, and the panel is placed in a copper etch, again for a carefully controlled amount of time.

6 Measurement

The first FSS panel size was approximately¡ 18 x 14 inches. Two identical FSS's were fabricated by Precision Prototypes of NJ, and delivered to JPL and the NRAO, Green Bank, respectively. Measurements were then made of the frequency response of the FSS by both JPL and NRAO. JPL used an indoor range, had the FSS sheet taped to a Rohacell foam backing, and used dielectric lenses mounted on the apertures of the test horns to focus the beam within the borders of the FSS, which was placed somewhere between the two test horns. JPL's indoor range allowed for swept frequency response measurements. NRAO used an outdoor range, with the FSS mounted within a wooden frame which was designed to stretch the FSS surface taut, and the wooden frame was bracketed approximately 10 inches in front of the receiving horn. The backup foam was placed behind the FSS to give more rigidity to the panel, but was not adhered to the FSS surface. For 7-12.5 GHz measurements, a circular corrugated X-band horn was used to receive, and for 13-16 GHz measurements, a pyramidal Ku-band horn was used. The NRAO does not have swept-frequency measurement capability, so data was taken repeatedly at discrete frequencies with a phase-locked receiver.

The test procedure was to measure the power received with nothing between the test horns. The FSS is then placed between the horns and the power measured for every desired incident angle typically 0°, 15°, 30° and 40°. The FSS is removed and the power again measured with nothing between the two test horns. The resulting difference between power received without and with the FSS is the insertion loss of the FSS.

The measurement results are summarized in Figures 3, 4, 5, and 6 below, with plots of NRAO and JPL measurements of FSS insertion loss versus frequency, as a function of incident angle and polarization. The correspondence between the predicted response shown in Figures 2, and the measured results in Figures 3–6 is good. For instance, the computer simulation predicted a 20 dB reflection bandwidth for TE incidence from 13.75–15.0 GHz. The measurement results were 13.75–15.0 GHz and 13.5–15.0 GHz for the NRAO and JPL measurements, respectively. Similar correspondence occurs at other angles and for both types of incident polarization. The exact bandwidths for the transmission band were difficult to discern due to the difficulty in measuring low levels of loss with the insertion loss setup. However, the band-center seemed to be about 8.1–8.3 GHz for each case, which is also close to the computer predicted results of 8.3–8.5 GHz.

For purposes of comparison, the graphs shown in Figures 7 were plotted, showing the results of computer simulation together with the measurement results for both TE and TM incidence at 30 degrees. The agreement is seen to be good between simulation and measurement, as the frequencies at which the simulated response has maxima and minima are only very slightly higher than measured values.

[6]Precision Prototypes, 55 Midland Ave., Garfield, NJ 07026

7 Discussion of Measurement Results

The results of the test of the first FSS, given in the previous section, did not meet our initial specifications. The specification was written rather simply, requiring better than 0.1 or 0.2 dB loss for certain frequency ranges, *for a range of angles of incidence and states of incident polarization.* We can tolerate losses at certain frequencies, angles, and polarization in excess of the levels given in the specification. We are currently studying the problem of what performance we really require from the FSS, as an overall efficiency term in the front-end and optics budget.

With the FSS placed in the near-field of a corrugated horn with circular polarization, many angles and a combination of TE and TM polarization are present at once. However, the total loss can be calculated by integrating the expected incident electric field, including amplitude, incident angle, and polarization, against the corresponding transmission or reflection loss function of the FSS. This has been done, using a program called FSSEFF written in FORTRAN on a SUN workstation. The results of this program, which uses measured FSS data, are shown in Fig. 8 for X-band and Ku-band. Clearly, the loss exceeds 0.2 dB for some frequencies between 7.2 GHz and 8.5 GHz; and exceeds 0.1 dB for some frequencies between 14.2 GHz and 15.3 GHz. The true efficiency is somewhat muddled in the "spikiness" of the X-band efficiency plot. This was caused by spurious reflections within the antenna range measuring system. Since the response of the FSS has an inherent shift with change in incident angle, we will generally attempt to use narrow beamwidth horns and small angle of incidence upon the FSS. Considerations such as these will be treated more fully in a future memo on the OVLBI optics.

Given these results, the bandwidth of the response, particularly at X-band, will not be enough to meet either the original specification or the overall efficiency specification.

However, there is a "fall-back" option, which would require the FSS only to diplex Radioastron downlink signals with high efficiency. This would require a mechanical structure on the antenna to be added so that the FSS can be remotely stowed for VSOP transmission. At present, the results of the overall efficiency study shown in Figures 2 and 3 indicate that the performance required at 8.47 GHz¡ and 15.063 GHz required for this option has already been met. In fact, if the design is scaled to effect a slight upward frequency shift, overall efficiency would be even better at these two frequencies. Significantly, this might achieve less than 0.1 dB loss at both 14.2 GHz and at 15.3 GHz. Thus, the only operational frequency at which the initial specification would not be met is at 7.2 GHz, where there would be about 1 dB of loss.

The loss calculations that we performed were done with certain assumptions that should be held in mind. First, transmission-only data was used. This means that the reflection loss was calculated assuming that all of the energy which was not *measured* in transmission was assumed to be reflected in the appropriate direction. Thus, we ignored the possible added loss of scattering loss and material loss.

8 Remaining Work

8.1 Tri-Layer FSS Design

We are presently trying to improve the design by using a layered teflon sandwich FSS. This approach was suggested to us by T.K. Wu. A copper pattern is etched on a teflon substrate, then another teflon layer of equal thickness is bonded over the copper pattern. The total thickness of the structure is approximately $\frac{\lambda}{8}$ at 15 GHz. The main objective is to reduce the amount that the Ku-band is dependent on incident angle. For the first FSS, at TM incidence, the 20 dB reflection bandwidth was 13.9-15.55 GHz for 0° and 13.2-14.1 GHz for 40° incidence. The 20 dB bandwidth of 13.9-14.1 GHz common to all angles between 0° and 40° was drastically insufficient. The 20 dB common bandwidth for TE incidence was 13.9-14.7 GHZ, slightly better. Initial computer simulations indicate that a design using two 30-35 mil layers of teflon on either side of the FSS reduces the downward shift of the TM response as the incident angle increases. The response of the tri-layer FSS structure was simulated by Wu, and the results are shown in Figure 9. The computer simulation results for this case are shown in Figure 10.

8.2 Reflection Measurements

Reflection measurements are needed to determine if Ku-band losses are as low as they appear. A limited amount of reflection testing has been done, with the result that the FSS appears to reflect nearly all the incident power at resonance, with loss < 0.1 dB. However, the angular alignment of the mirror-FSS was not precisely done, and more reflection measurements are needed. Even more realistic reflection conditions can be measured, of course, once the subreflector and ellipsoid are procured.

8.3 Implementation of New FSS simulation program

A major difficulty has been the lack of an adequate FSS simulation program at the NRAO. Lumped element models have been written and are accurate to within about 300 MHz at 15 GHz, but do not predict reliably the polarization and angular effects. There exists an FSS simulation code from Ohio State University which we are trying to obtain, but it is taking longer than expected.

8.4 Measurement of FSS

We should spare no more time in fabricating and measuring the tri-layer FSS. A parallel effort is underway to develop a computer-controlled swept-frequency measurement setup for making FSS measurements on the antenna range.

8.5 Consideration of Cross-Polarization Effects

Cross-polarization effects are introduced in our type of optics by two factors. First, the FSS elements convert some energy between orthogonal polarizations. Previous studies by Langley and Lee[7] were done on a gridded-double-square array (the same as a gridded-square array, but with an additional resonant loop within the first resonant loop). They measured levels of cross-polarization at 45-degrees incidence on their FSS in both transmission and reflection. Im measurements with and without the FSS, they found that the peak level of cross-polarization rose from -37 dB to -34 dB in transmission and -40 to -37 dB in reflection. This would be a very acceptable figure for our purposes. We should investigate whether these figures would be valid for the proposed tri-layer FSS. The second contribution to cross-polarization is from the offset geometry. These effects need to be quantified and expressed as a polarization loss.

8.6 Development of low-vibration frame

The two-way timing link can be compromised by an FSS that is not mechanically sound, due to path-length variations. Design of a sufficiently stiff supporting structure has not yet been attempted.

8.7 Optimization of Material

Environmental factors, particularly temperature variation, will alter the frequency response of the FSS. Typical woven teflon materials, including the one chosen for the next fabrication (Norplex Oak 602 microwave substrate), have low coefficient of thermal expansion across the face of the panel, so that the element size would not change much. However, the thermal expansion coefficient for the thickness dimension is 150 $\frac{\text{ppm}}{^\circ\text{C}}$. This may be prohibitively large, requiring a more temperature-stable material to be found.

9 Acknowledgement

We would like to acknowledge the valuable consulting help we received from Dr. T.K. Wu of JPL. He was contracted for the initial FSS design, and proposed the use of a gridded-square array element. He also selected the dimensions of the prototype FSS and made the measurements shown in Figures 5 and 6. Lending us the benefit of his experience in FSS design, he provided valuable advice concerning choice of materials and answered many questions of a more general nature.

He also suggested the tri-layer FSS approach as a possible next step in the optimization of our FSS frequency response. He simulated the tri-layer FSS with same dimensions as the original FSS, then scaled the dimensions so that the frequency response of the tri-layer FSS met our specified frequency band.

[7]R.J. Langley and C.K. Lee, "Design of Single-Layer Frequency Selective Surfaces for Multiband Reflector Antennas," Electromagnetics, May, 1985, pp. 331-347

FSS FABRICATION SPECIFICATION

1. Part No. GS1

2. Grided square loop patch element array centered in 18" by 18" flat Kapton sheet.

5. The kapton sheet is 3 mil thick and the one-sided copper cladding is less than 0.5 mil thick.

6. The grided square loop element array is symmetric in both x and y directions as illustrated in the following figure. The line dimensions are given as follows;

P=0.3543"

W1=g=0.022"

W2=0.0443"

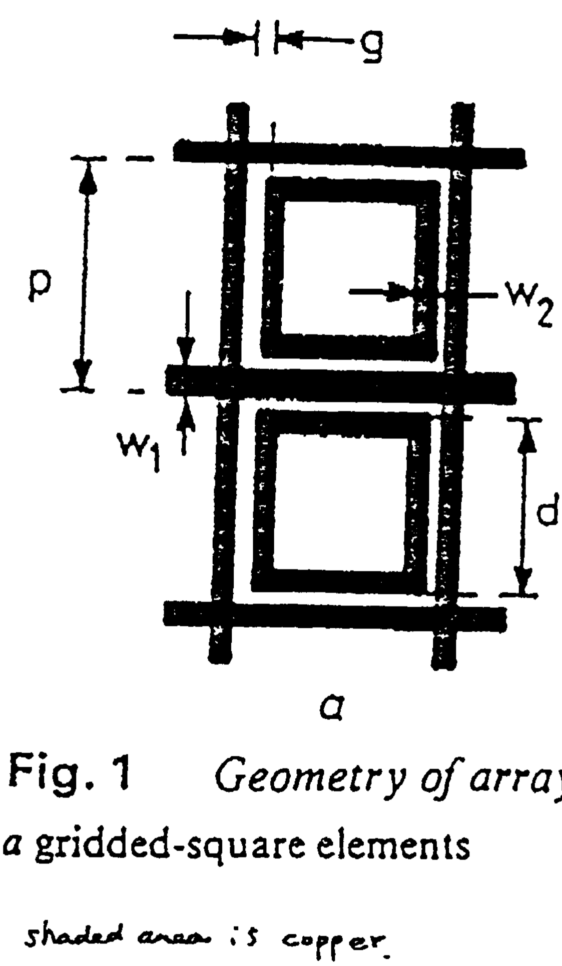

Fig. 1 *Geometry of arrays*

a gridded-square elements

shaded area is copper.

Fig. 1: Geometry and dimensions of FSS element

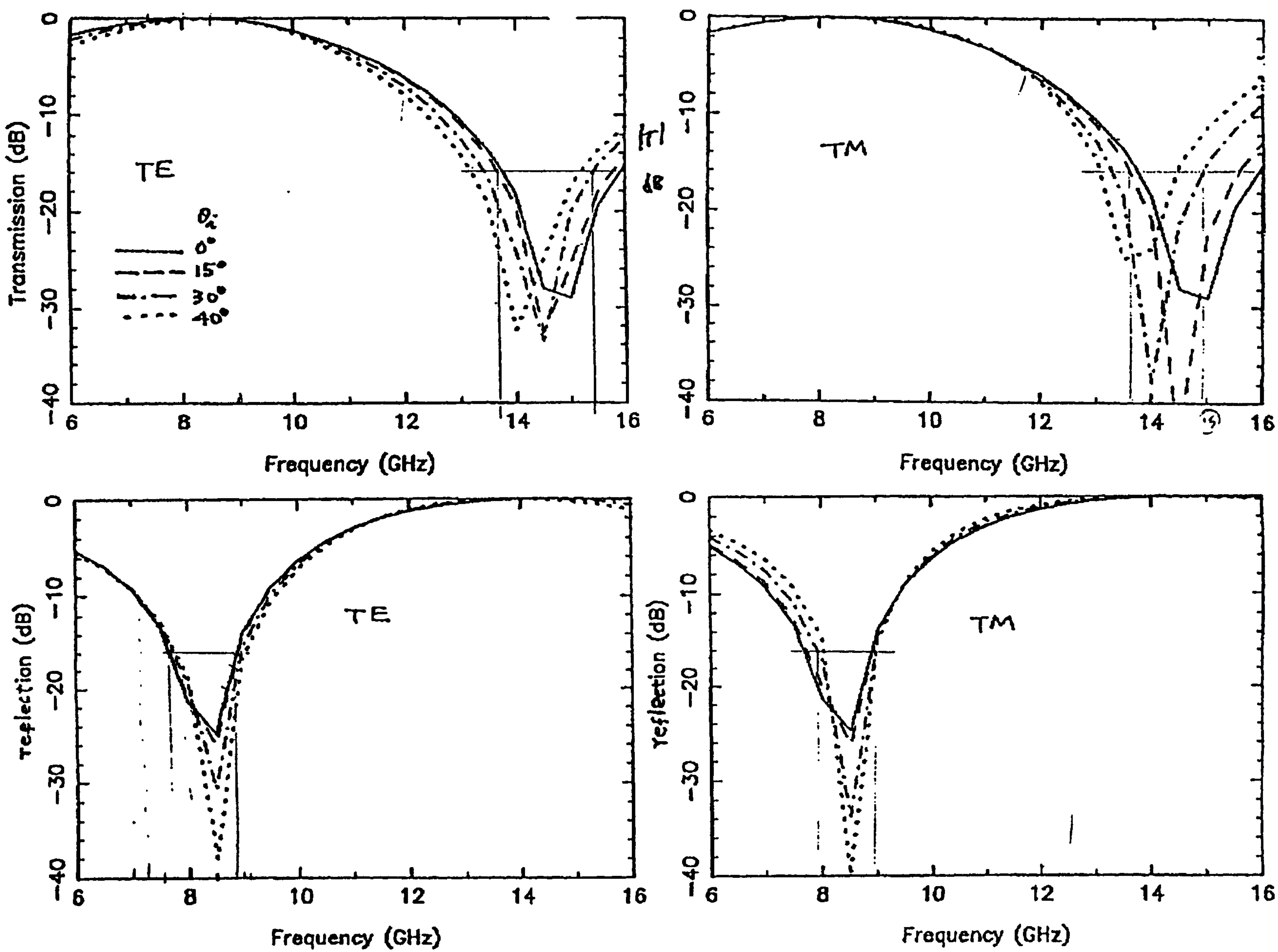

Fig. 2: Computer simulation of transmission and reflection response of FSS for TE and TM incidence.
By T.K. Wu, JPL.

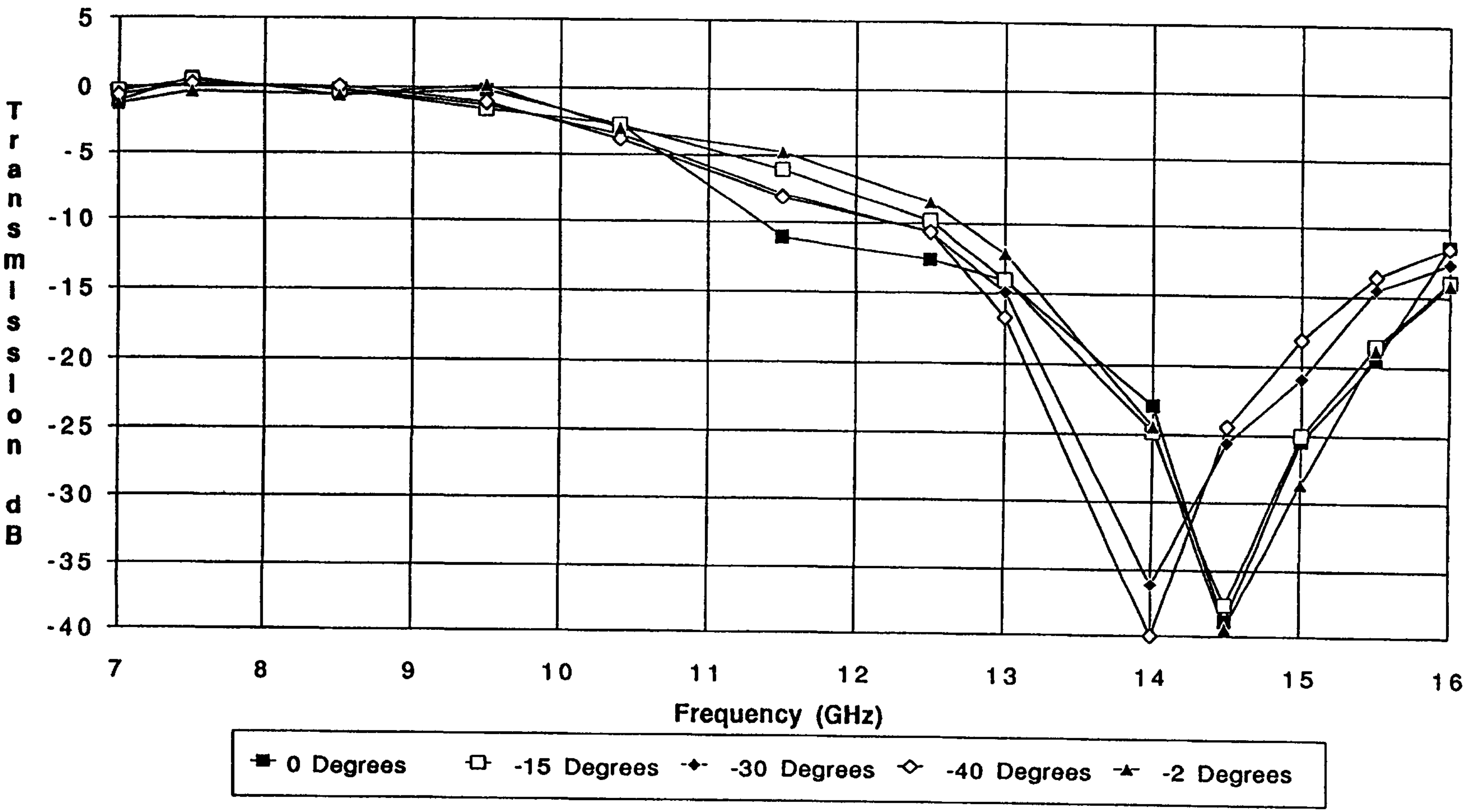

Fig. 3: NRAO measurement results for TE incidence

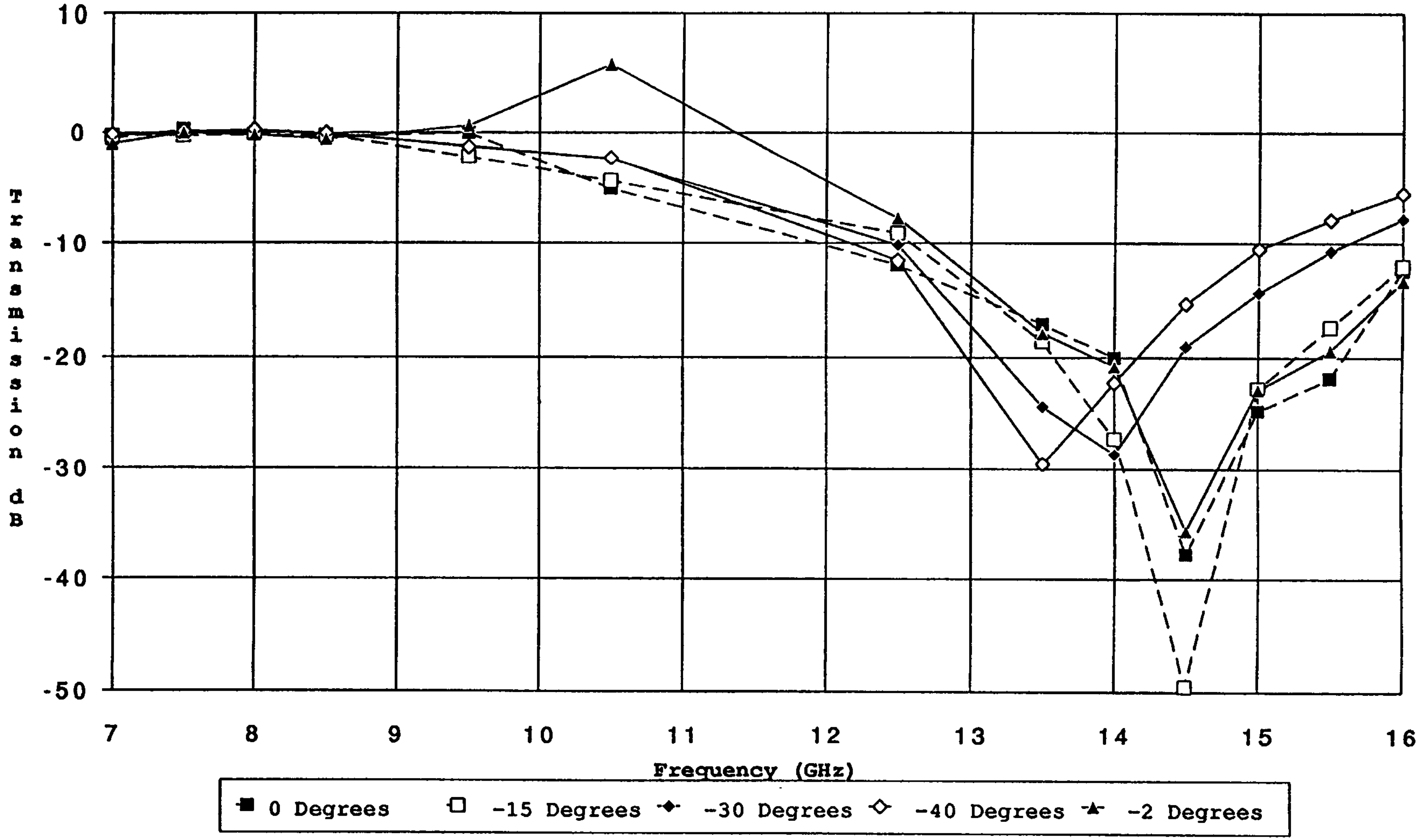

Fig. 4: NRAO measurement results for TM incidence

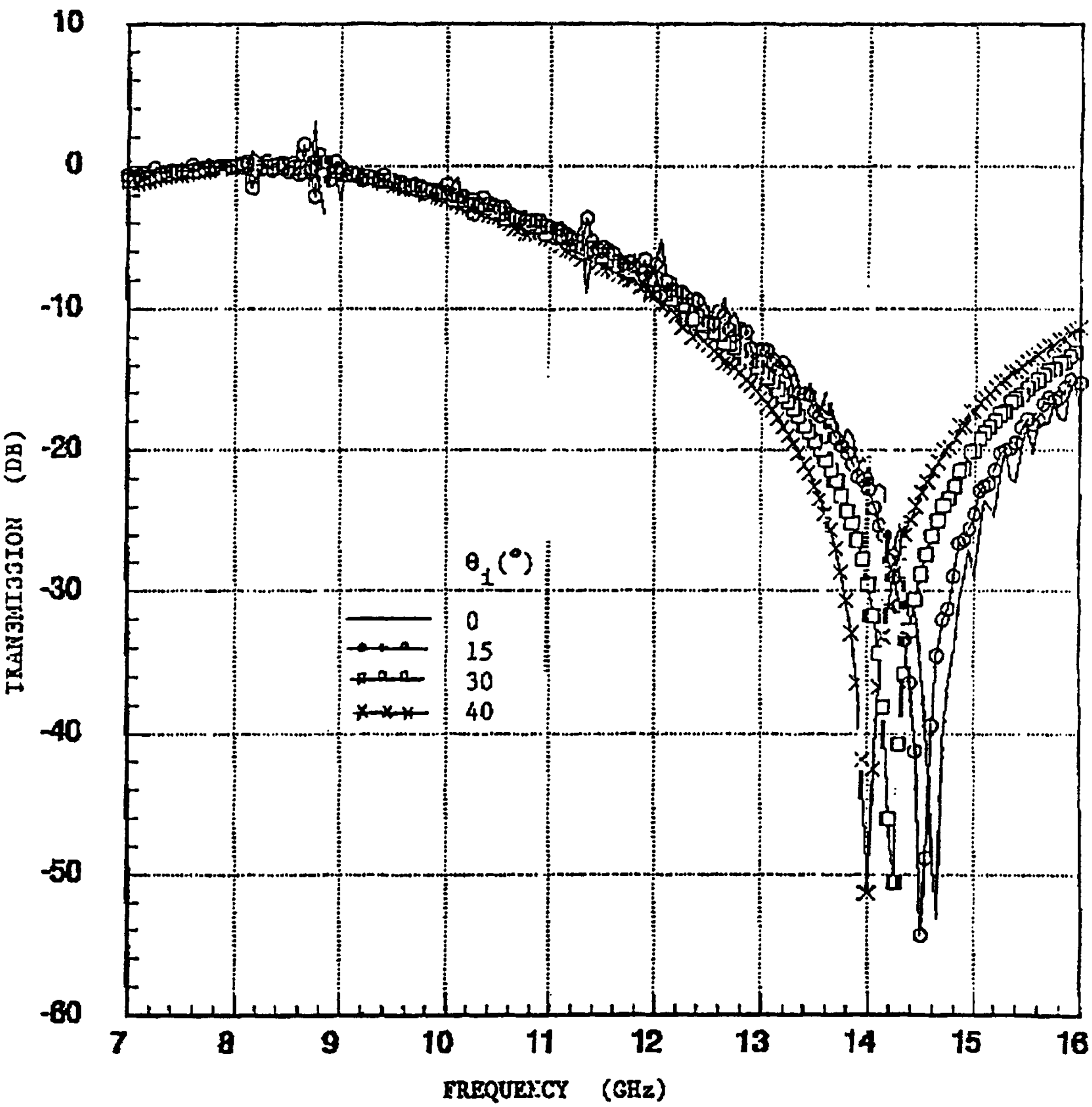

Fig. 5: JPL measurement results for TE incidence

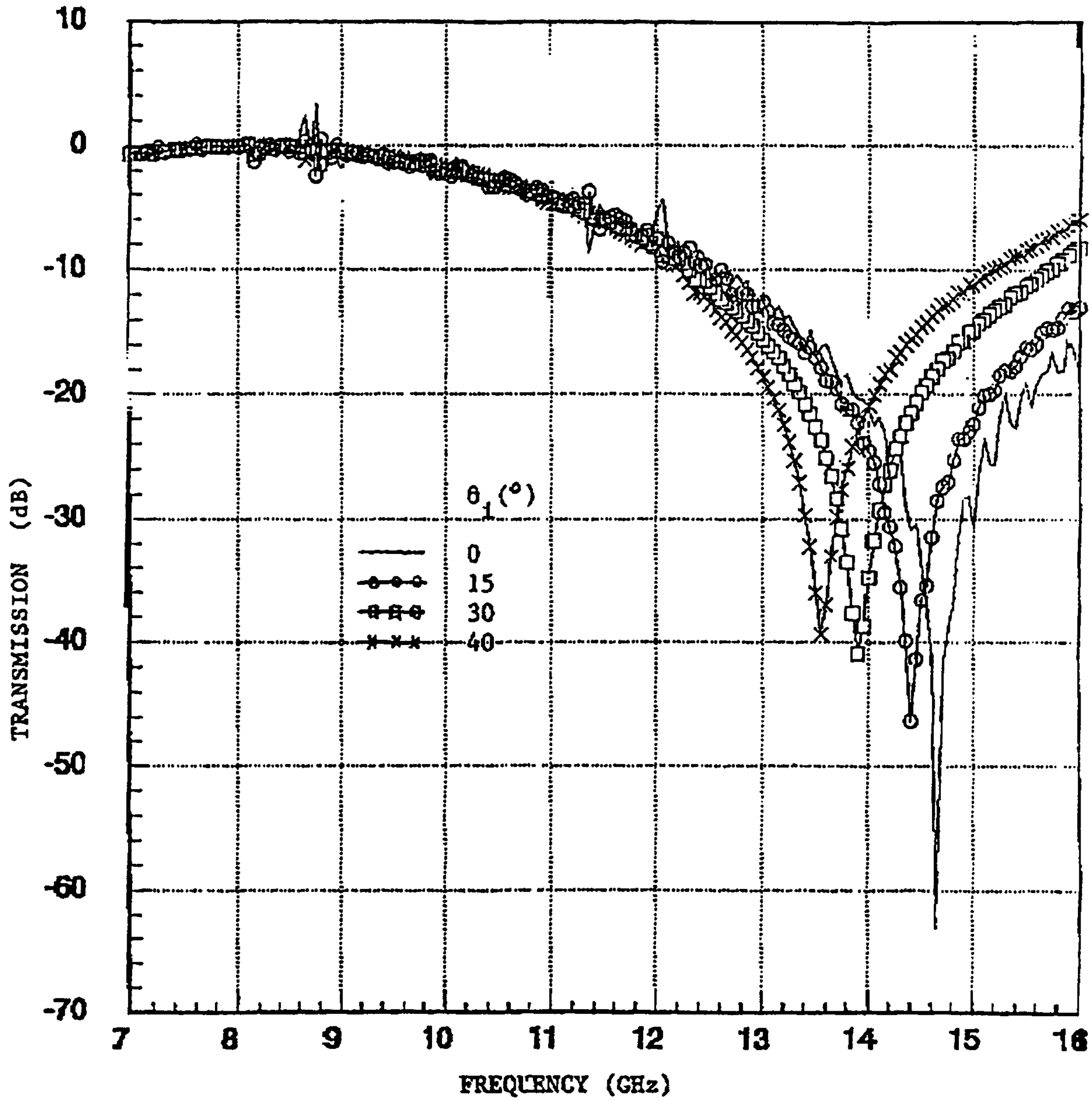

Fig. 6: JPL measurement results for TM incidence

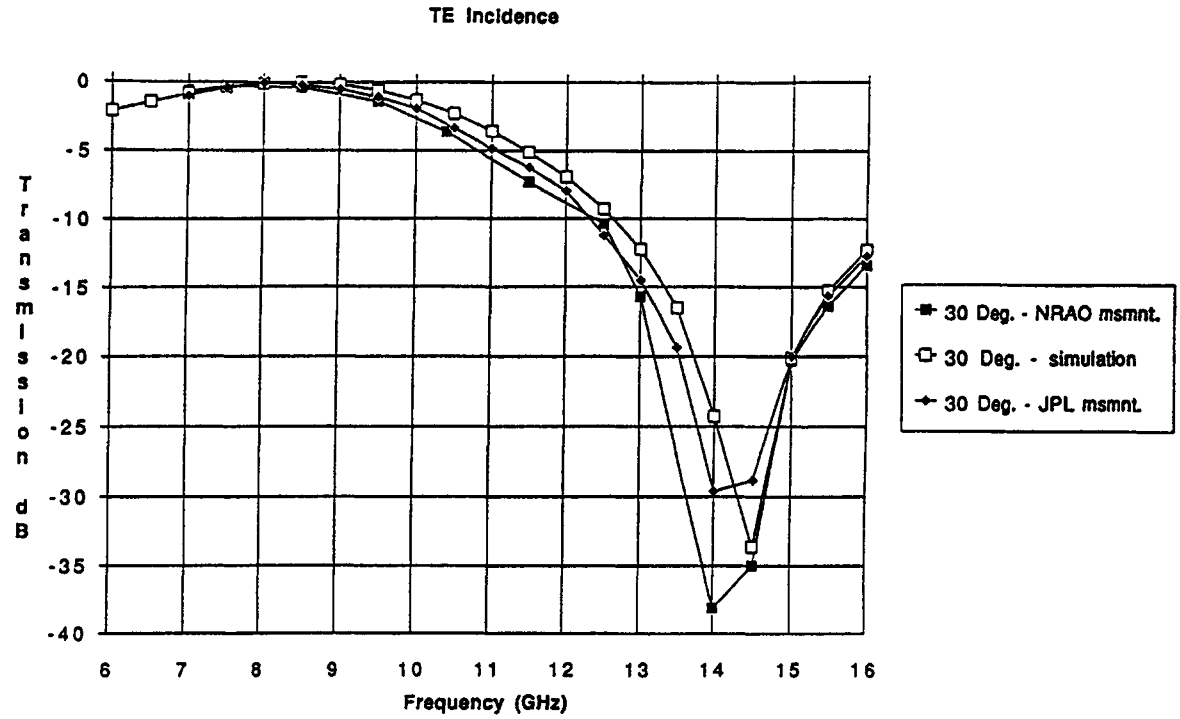

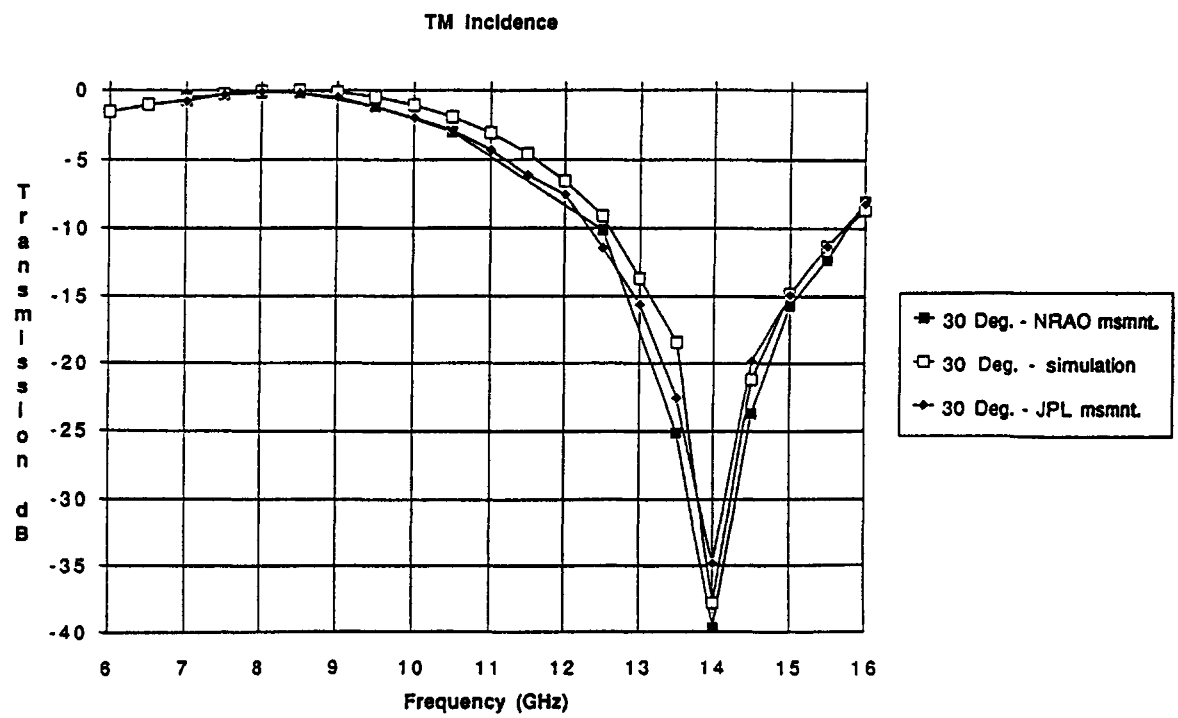

- Fig. 7: Computer simulation results (from Fig. 2) and measurement results (from Figs. 3–6) at 30° for both TE and TM incidence

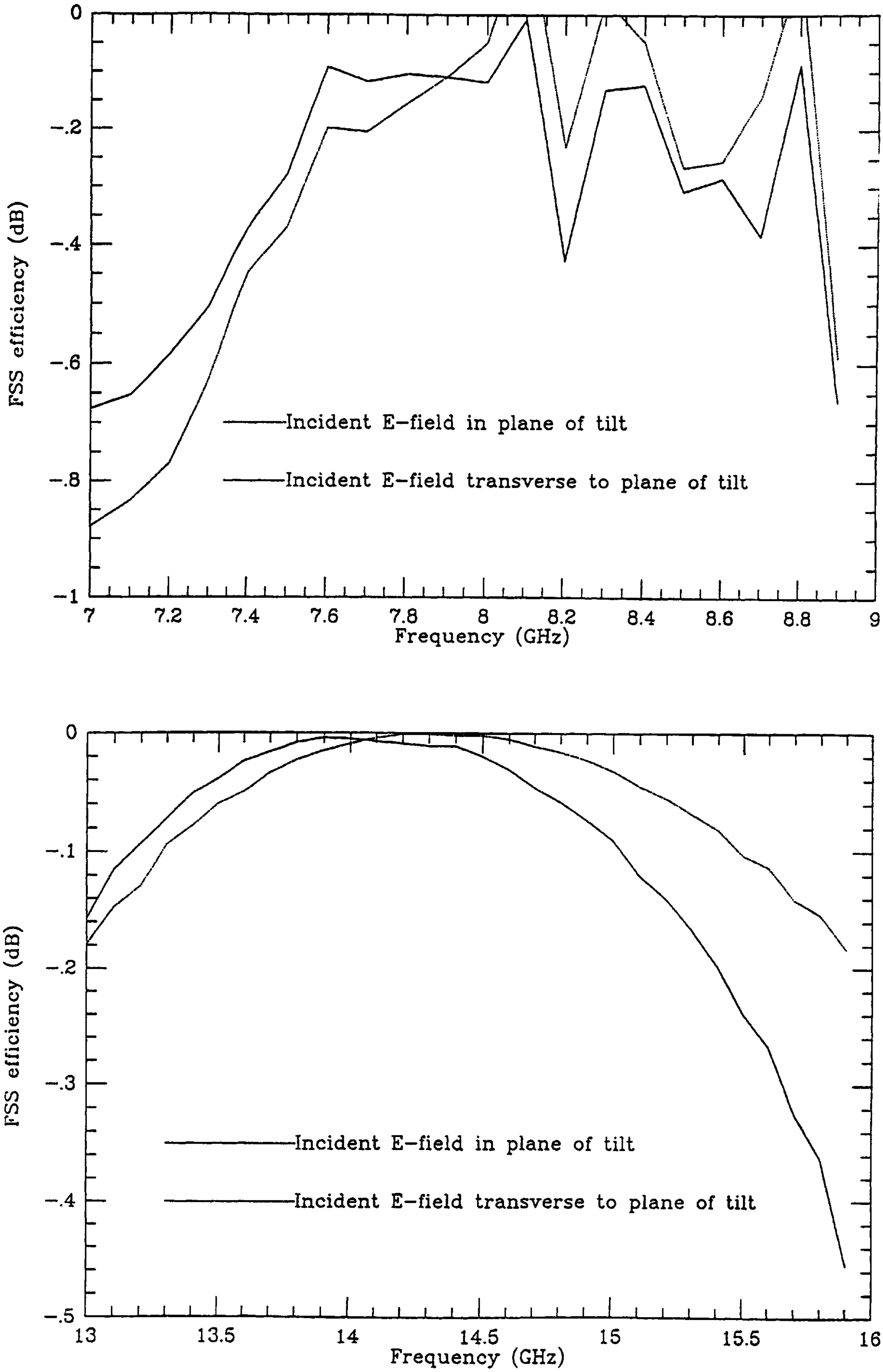

Fig. 8: Results of computation of overall efficiency for FSS in X-band and Ku-band. Program used JPL measured data.

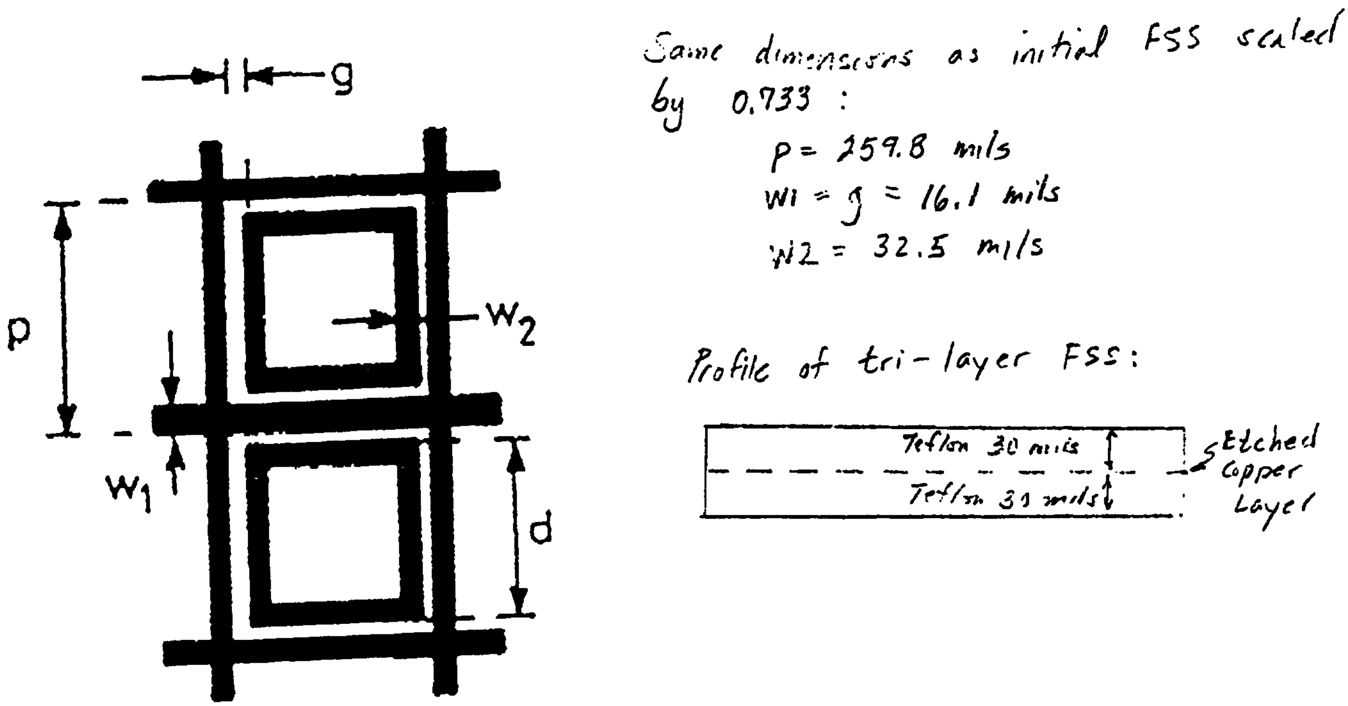

Fig. 9: Geometry and dimensions of tri-layer FSS

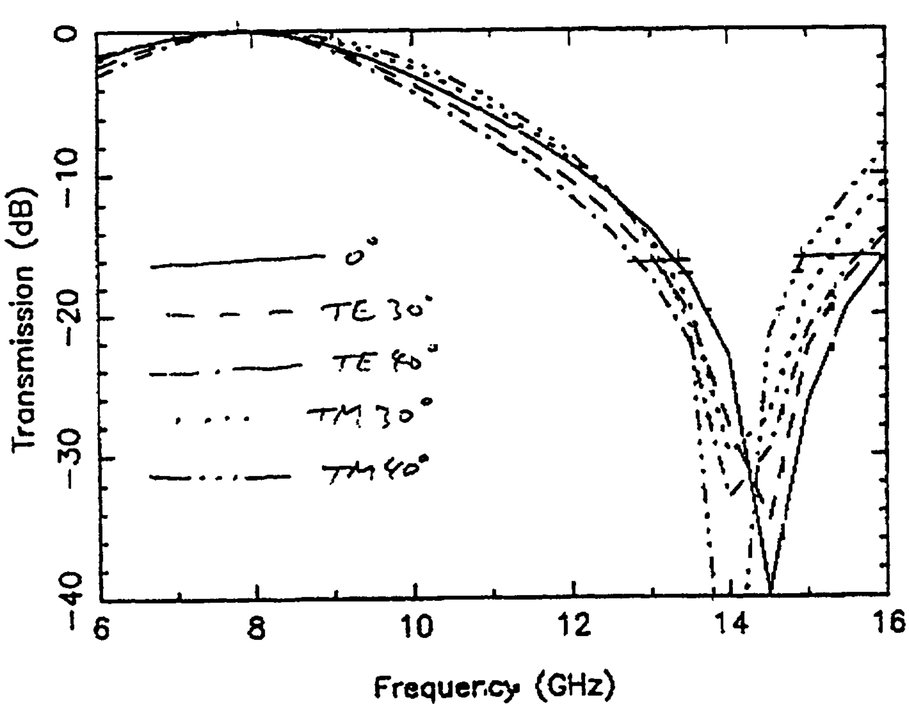

Fig. 10: Simulation results for transmission response of tri-layer FSS for TE and TM incidence